

**(*p,d*) Reactions with  ${}^6\text{Li}$ ,  ${}^7\text{Li}$ , and  ${}^9\text{Be}^\dagger$** 

L. A. KULL

*Cyclotron Laboratory, Michigan State University, East Lansing, Michigan*

(Received 27 March 1967; revised manuscript received 22 May 1967)

Excited states of  ${}^6\text{Li}$ ,  ${}^7\text{Li}$ , and  ${}^9\text{Be}$  were studied by means of the (*p,d*) reaction, using 33.6-MeV incident protons. Deuteron groups were observed corresponding to strongly excited levels in  ${}^6\text{Li}$  at 0.0 and 16.6 MeV; in  ${}^7\text{Li}$  at 0.0, 2.15, 3.57, and 5.38 MeV; and in  ${}^9\text{Be}$  at 0.0, 3.1, 11.4, 16.95, 17.62, 18.18, and 19.21 MeV. Small deuteron yields were observed for excited levels of  ${}^9\text{Be}$  at 16.6 and 19.15 MeV. Angular distributions were taken for the strongly excited states, and the results were compared with a distorted-wave Born-approximation (DWBA) calculation. Angular distributions for the elastic scattering of 33.6-MeV protons from targets of  ${}^6\text{Li}$ ,  ${}^7\text{Li}$ , and  ${}^9\text{Be}$  were measured and fitted with an optical-model calculation to obtain the proton optical parameters used in the DWBA analysis. With a few exceptions, which are discussed, the (*p,d*) angular distributions are characteristic of a direct pickup of a *1p*-shell neutron. Spectroscopic factors were extracted from the experimental data and were compared with those obtained from theoretical intermediate-coupling calculations in the *1p* shell. The results are discussed for the high excited states of  ${}^9\text{Be}$ , where isotopic-spin mixing is indicated.

**INTRODUCTION**

**T**HIS paper describes the results of (*p,d*) reactions on  ${}^6\text{Li}$ ,  ${}^7\text{Li}$ , and  ${}^9\text{Be}$  with 34-MeV protons.<sup>1</sup> Previous studies of the (*p,d*) reaction on these nuclei have been made at Princeton University with an incident proton energy of approximately 18 MeV in which only the lower excited states of the residual nuclei could be observed.<sup>2-4</sup> The same reactions were also studied at the University of Minnesota using 40-MeV protons,<sup>5,6</sup> where a magnetic spectrometer was used to measure angular distributions out to 40° for most of the lower excited states of the residual nuclei. Many other studies of these reactions have been done at even lower proton energies, most of which examined the properties of the ground state and lower excited states of  ${}^6\text{Li}$ ,  ${}^7\text{Li}$ , and  ${}^9\text{Be}$ .<sup>7</sup> The (*p,d*) reactions on these nuclei have also been investigated with incident proton energies of 95 MeV and above.<sup>8-10</sup> The range of observable excitation energy in the residual nuclei included all the known strongly excited levels; however, the energy resolution did not permit the separation of closely spaced levels.

The purpose of this work was to use an incident proton beam with sufficient energy to allow observation of all the strongly excited levels in  ${}^6\text{Li}$ ,  ${}^7\text{Li}$ , and  ${}^9\text{Be}$ , and yet with a low enough energy to enable the use of solid-state detectors with their desirable resolution

capabilities. An incident proton energy of about 34 MeV fulfilled both requirements. The data were analyzed to extract spectroscopic factors using a method successfully applied to (*p,d*) reactions with medium weight nuclei.<sup>11,12</sup> The experimental results were then compared to the theoretical intermediate coupling calculations in the *1p* shell of Kurath<sup>13</sup> and of Barker.<sup>14</sup>

**EXPERIMENTAL DETAILS****General**

Negative hydrogen ions were accelerated by the Michigan State University sector-focused isochronous cyclotron to an energy of 33.6 MeV, and a proton beam was extracted by means of a 700- $\mu\text{g}/\text{cm}^2$  aluminum stripping foil.<sup>15</sup> Single turn extraction was obtained with a beam spread of  $\sim 0.1\%$ ; over-all energy resolution in the deuteron spectra of 100 to 130 keV can then be achieved as is seen in the sample  ${}^{12}\text{C}(p,d){}^{11}\text{C}$  spectrum in Fig. 1. The proton beam energy was determined by the kinematic crossover method<sup>16</sup> and by an independent range-energy calibration. Results from both methods agree to within an experimental uncertainty of 200 keV.

The extracted proton beam was focused on a collimator at the entrance of a 36-in. scattering chamber by means of two quadrupole magnets and a 20° bending magnet. The dimensions of the beam on the target were approximately 0.25-in. high and 0.12-in. wide. A beam which passed through the target was collected at the rear of the scattering chamber in a Faraday cup, and the collected charge was integrated and measured by a current integrator which was calibrated and

\* Work supported in part by the National Science Foundation.

<sup>1</sup> L. A. Kull, *Bull. Am. Phys. Soc.* **12**, 17 (1967).

<sup>2</sup> J. G. Likely, *Phys. Rev.* **98**, 1538A (1955).

<sup>3</sup> J. B. Reynolds and K. G. Standing, *Phys. Rev.* **101**, 158 (1956).

<sup>4</sup> E. F. Bennett and D. R. Maxson, *Phys. Rev.* **116**, 131 (1959).

<sup>5</sup> T. H. Short and N. M. Hintz, *Bull. Am. Phys. Soc.* **9**, 391 (1964).

<sup>6</sup> University of Minnesota Linac Laboratory Progress Report, No. 61, 1964 (unpublished).

<sup>7</sup> T. Lauritsen and F. Ajzenburg-Selove, *Nucl. Phys.* **78**, 1 (1966).

<sup>8</sup> W. Selove, *Phys. Rev.* **101**, 231 (1956).

<sup>9</sup> D. Bachelier *et al.*, *J. Phys. (Paris) Colloq.* **1**, 70 (1966).

<sup>10</sup> D. Bachelier *et al.*, International Conference on Nuclear Physics, Gatlinburg, 1966 (unpublished).

<sup>11</sup> E. Kashy and T. W. Conlon, *Phys. Rev.* **135**, B389 (1964).

<sup>12</sup> R. Sherr *et al.*, *Phys. Rev.* **139**, B1272 (1965).

<sup>13</sup> D. Kurath (private communication).

<sup>14</sup> F. C. Barker, *Nucl. Phys.* **83**, 418 (1966).

<sup>15</sup> M. E. Rickey and R. Smythe, *Nucl. Instr. Methods* **18**, 19, 66 (1962).

<sup>16</sup> B. M. Bardin and M. E. Rickey, *Rev. Sci. Instr.* **35**, 902 (1964).

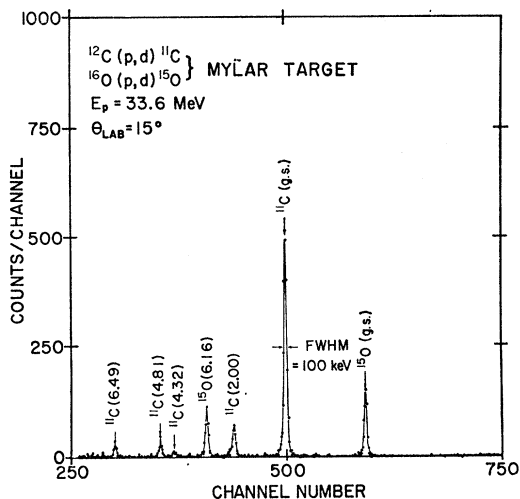


FIG. 1.  ${}^{12}\text{C}(p,d){}^{11}\text{C}$  deuteron spectrum at  $15^\circ$ . The target was a  $1.03\text{-mg/cm}^2$  Mylar foil; this thickness represents  $\sim 45\text{-keV}$  energy loss to  $19\text{-MeV}$  deuterons. Over-all energy resolution in the neighborhood of  $100\text{ keV}$  is indicative of single turn extraction as the individual turns are separated by  $\sim 80\text{ keV}$ .

checked to be accurate to better than  $1\%$ . The beam current was varied from  $1\text{--}60\text{ nA}$ , depending on the angle at which the counters were placed relative to the beam.

The counters were mounted on an arm which could be remotely positioned to an angular accuracy of  $\pm 0.4^\circ$ ; the target angle was determined to within  $\pm 2^\circ$ . Counters were mounted in a  $\Delta E\text{--}E$  counter telescope configuration. The  $\Delta E$  counter was a silicon surface barrier detector whose selected thickness varied between  $150$  and  $770\ \mu$ , depending on the particular target in use and on the counter arm angle; the  $E$  counter was a lithium-drifted silicon detector with a nominal thickness of  $3\text{ mm}$ . With this system, deuterons with energies from  $7$  to  $35\text{ MeV}$  could be detected and identified. The angle subtended by the counter in the scattering plane was  $1^\circ$  or less.

Pulses from the  $E$  and  $\Delta E$  detectors were amplified and routed to a Goulding particle identification system.<sup>17</sup> The resulting deuteron spectra were stored in a  $4096\text{-channel}$  analyzer. For the particular case of  ${}^7\text{Li}(p,d){}^6\text{Li}$ , the energy resolution for the entire system was  $125\text{ keV}$ , the major portions of which were electronic noise ( $\sim 70\text{ keV}$ ) and target thickness ( $\sim 75\text{ keV}$ ).

The experimental apparatus used for the measurement of elastically scattered protons was similar to that described above for  $(p,d)$  reactions with the following exceptions. A cylindrically shaped cesium iodide crystal,  $0.5\text{-in.}$  long and  $0.25\text{ in.}$  in diameter, mounted on a photomultiplier tube was used as the proton detector. The over-all energy resolution obtained for these measurements was approximately  $500\text{ keV}$ .

<sup>17</sup> F. S. Goulding, D. A. Landis, J. Cerny, and R. H. Pehl, Nucl. Instr. Methods **31**, 1 (1964).

## Targets

The  ${}^6\text{Li}$  targets were made by rolling isotopically enriched lithium ( $99.32\%$   ${}^6\text{Li}$ ) to a thickness of approximately  $1.8$  to  $1.9\text{ mg/cm}^2$ . Except for brief periods of exposure to air, the targets were kept in a vacuum or in an argon atmosphere to avoid oxygen and nitrogen contamination. The  ${}^7\text{Li}$  targets were similarly fabricated from isotopically enriched lithium ( $99.993\%$   ${}^7\text{Li}$ ) with thicknesses of about  $2.3\text{ mg/cm}^2$ . The  ${}^9\text{Be}$  target was commercially purchased  $2.06\text{-mg/cm}^2$  foil of natural beryllium ( $100\%$   ${}^9\text{Be}$ ). These thicknesses represent an energy loss of  $60\text{--}75\text{ keV}$  for  $30\text{-MeV}$  deuterons.

## EXPERIMENTAL RESULTS

### ${}^6\text{Li}(p,d){}^5\text{Li}$

Figure 2 is a deuteron energy spectrum taken at  $\theta_{\text{lab}}=15^\circ$  showing deuteron groups corresponding to the ground state ( $J^\pi=\frac{3}{2}^-$ ) and  $16.65\text{-MeV}$  state ( $J^\pi=\frac{3}{2}^+$ ) of  ${}^5\text{Li}$ . The location of the broad ground state of  ${}^5\text{Li}$  ( $\Gamma=1.3\text{--}1.4\text{ MeV}$ ) just above the  $\alpha+p$  separation energy (Fig. 3) is an inducement to use a simple cluster model<sup>18</sup> description of the state, consisting of an  $\alpha$  particle coupled to a proton with orbital angular momentum  $l=1$ . Possible spin and parity assignments for this configuration are  $\frac{3}{2}^-$  and  $\frac{1}{2}^-$ . A very broad  $\frac{1}{2}^-$  level ( $\Gamma=3\text{--}5\text{ MeV}$ ) has been reported at an excitation energy of  $5$  to  $10\text{ MeV}$ .<sup>7</sup> A deuteron group corresponding to this level has not been identified in the energy spectra, but because of its large width, it may be impossible to isolate it from the background due to three-body breakup. It is also possible that a significant fraction of the yield of this  $\frac{1}{2}^-$  level lies below  $5\text{-MeV}$  excitation energy, and that the deuterons corresponding

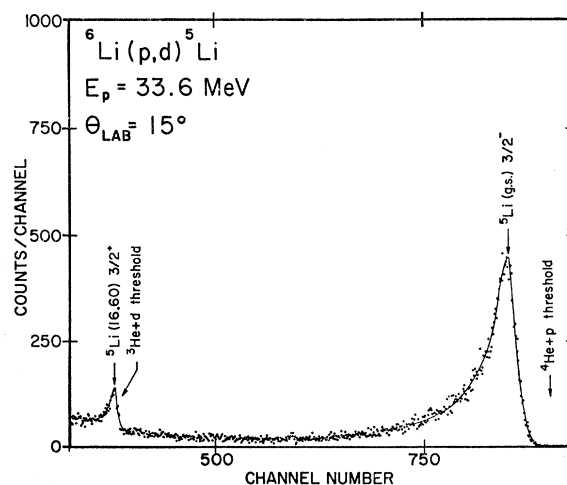


FIG. 2.  ${}^6\text{Li}(p,d){}^5\text{Li}$  deuteron spectrum at  $15^\circ$ . The long tail on the ground-state peak may include a contribution from a previously reported  $J^\pi=\frac{1}{2}^-$  state.

<sup>18</sup> K. Wildermuth and Th. Kanellopoulos, Nucl. Phys. **1**, 150 (1958).

to this state have been included in the tail of the ground-state peak.

No other levels have been reported<sup>4</sup> below the relatively narrow ( $\Gamma=360$  keV) 16.6-MeV state which lies just above the  ${}^3\text{He}+d$  separation energy as shown in Fig. 3. There, in a situation analogous to that of the ground state, a simple cluster-model description consisting of a  ${}^3\text{He}$  nucleus coupled to a deuteron with  $l=0$  seems appropriate for this state. The above configuration allows  $J^\pi$  values of  $\frac{3}{2}^+$  and  $\frac{1}{2}^+$ .

The 16.6-MeV level of  ${}^5\text{Li}$  ( $J^\pi=\frac{3}{2}^+$ ) was strongly excited in this reaction and a search was made in the vicinity of this peak in order to detect the presence

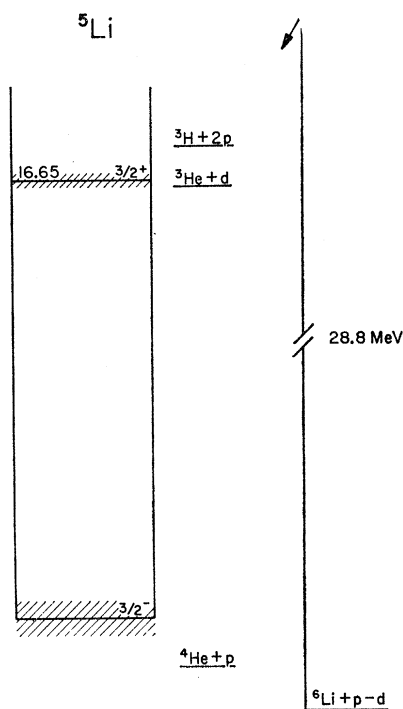


FIG. 3. Energy-level diagram of  ${}^5\text{Li}$ . Only the states observed in the  ${}^6\text{Li}(p,d){}^5\text{Li}$  reaction are shown and the excitation energies listed are those given in Ref. 7.

of the  $\frac{1}{2}^+$  member of the doublet. Various incident proton energies were tried between 30 and 40 MeV, as this was the experimentally obtainable range of energies where the available phase space for competing three-body breakup was calculated to be smallest.<sup>19</sup> No evidence was found that would locate the excitation energy of the  $\frac{1}{2}^+$  level. There was also no indication that a  $(\frac{3}{2}, \frac{5}{2})^+$  state previously reported at 20-MeV excitation is excited in this reaction.<sup>20</sup>

Figure 4 shows a comparison of the angular distributions for the reaction  ${}^6\text{Li}(p,d){}^5\text{Li}$  (g.s.) calculated using

<sup>19</sup> I. L. Rozental, Zh. Eksperim. i Teor. Fiz. **28**, 118 (1955) [English transl.: Soviet Phys.—JETP **1**, 166 (1955)].

<sup>20</sup> T. A. Tombrello, A. D. Bacher, and R. J. Spiger, Bull. Am. Phys. Soc. **10**, 423 (1965).

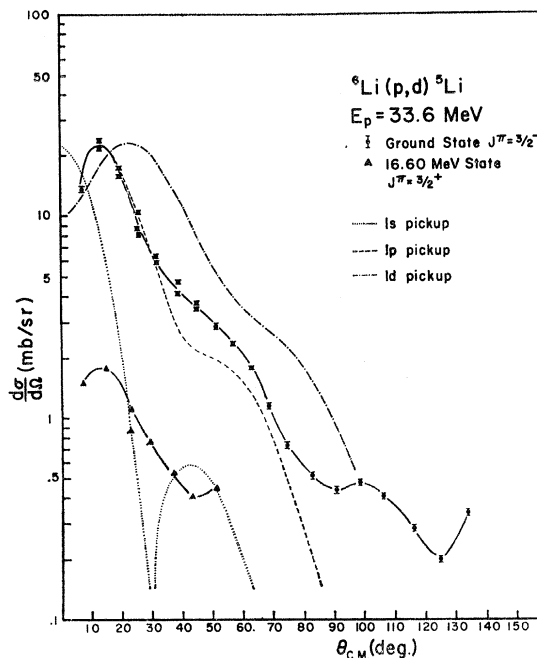


FIG. 4.  ${}^6\text{Li}(p,d){}^5\text{Li}$  angular distributions. The error bars shown only represent the uncertainty due to statistics and the solid lines are drawn to guide the eye. Results from DWBA calculations for the ground state differential cross section are shown assuming the neutron was picked up from the  $1s$ ,  $1p$ , and  $1d$  shells.

the distorted wave Born approximation assuming the neutron was picked up from the  $1s$ ,  $1p$ , and  $1d$  shells (orbital angular momenta  $l_n=0, 1$ , and  $2$ , respectively). In the same figure it can be seen that the experimental angular distribution for the ground state of  ${}^5\text{Li}$  shows a characteristic shape for transfer of a neutron from the  $1p$  shell ( $l_n=1$ ) by a direct reaction mechanism (Fig. 4). The angular distribution for the 16.6-MeV state could not be obtained for lab angles greater than

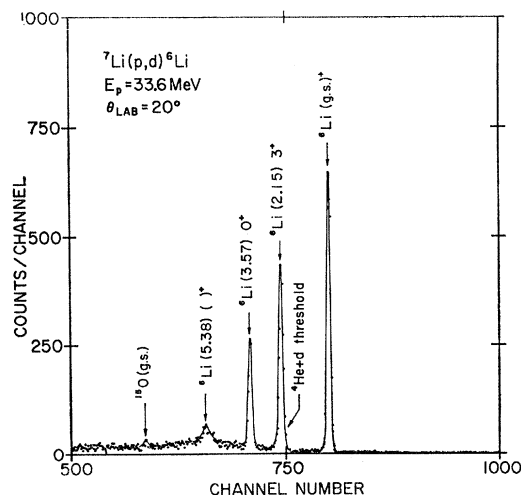


FIG. 5.  ${}^7\text{Li}(p,d){}^6\text{Li}$  deuteron spectrum at  $20^\circ$ . A small peak due to  $\sim 1.5\%$  oxygen contamination can be seen.

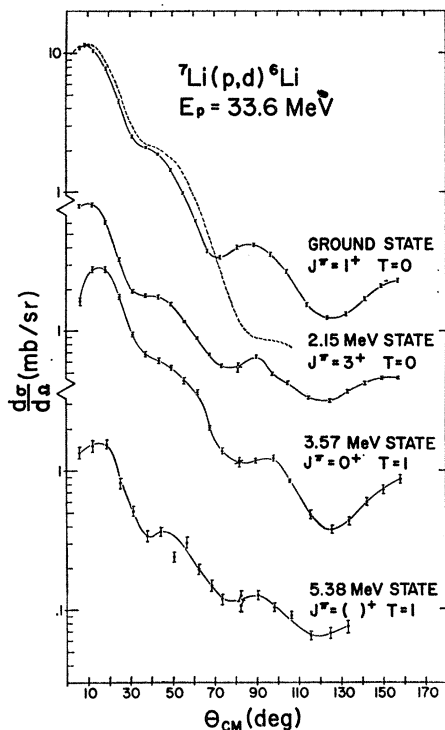


FIG. 6.  ${}^7\text{Li}(p,d){}^6\text{Li}$  angular distributions. The DWBA fit to the ground-state differential cross section is shown by a dashed line.

$35^\circ$  because the deuteron peak could not be distinguished from a strong background due to three-body breakup. This state is excited by the pickup of a  $1s$  neutron from  ${}^6\text{Li}$  but, because of the small amount of data, little can be said concerning the shape of the angular distribution.

#### ${}^7\text{Li}(p,d){}^6\text{Li}$

Four deuteron groups were observed in the energy spectra from the  ${}^7\text{Li}(p,d){}^6\text{Li}$  reaction corresponding to

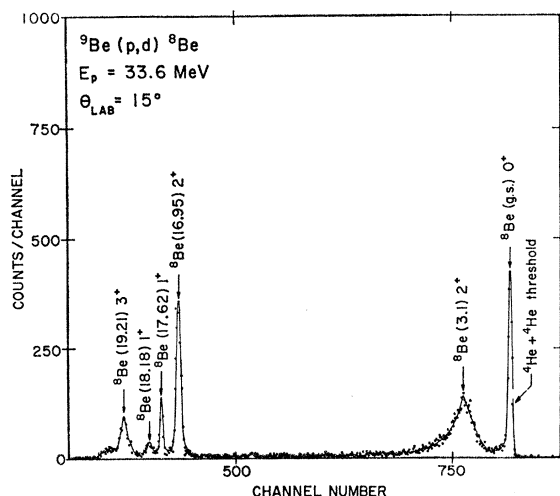


FIG. 7.  ${}^9\text{Be}(p,d){}^8\text{Be}$  deuteron spectrum at  $15^\circ$ .

states of  ${}^6\text{Li}$  at 0.0-, 2.15-, 3.57-, and 5.38-MeV excitation energy (Fig. 5). A small peak corresponding to the ground state of  ${}^{16}\text{O}$  indicates the presence of a small amount of oxygen contamination on the target (less than 1.5%). No evidence for any other strongly excited states was found up to 18 MeV of excitation energy for  ${}^6\text{Li}$ . Deuteron groups corresponding to the positive parity states of  ${}^6\text{Li}$  at 4.57 and 6.0 MeV were not observed; however, these states are broad and if weakly excited the peaks would be difficult to extract from the background. The shapes of the angular distributions for the 0.0-, 2.15-, 3.57-, and 5.38-MeV states are characteristic of  $l_n=1$  pickup (Fig. 6). This fixes the relative parity between the initial and final states<sup>21</sup>; in particular, this assigns a positive parity to the 5.38-MeV level. A positive parity fits in with the tentative  $T=1$  isospin assignment<sup>7</sup> for this state and places it in the isospin multiplet of which 1.80-MeV state of  ${}^6\text{He}$  [ $J^\pi=(2)^+$ ] is a member.

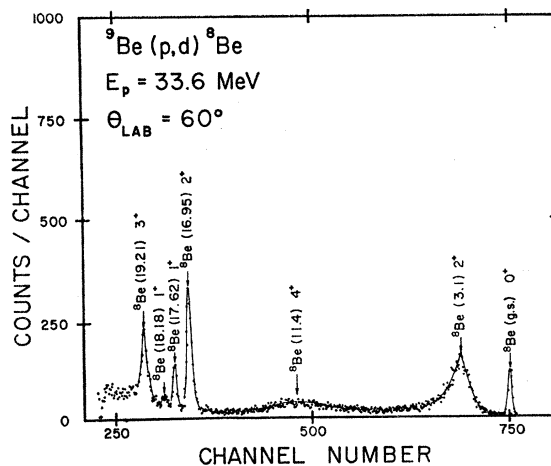


FIG. 8.  ${}^9\text{Be}(p,d){}^8\text{Be}$  deuteron spectrum at  $60^\circ$ . The broad peak corresponding to the 11.4-MeV level of  ${}^8\text{Be}$  can be clearly seen at back angles where its yield is comparable to that of the narrower levels.

It is interesting to note that the slopes of the first peak of the angular distributions for the  $T=0$  states at 0.0 and 2.15 MeV are much steeper than those of the lowest  $T=1$  states at 3.57 and 5.38 MeV. This may have some implication concerning the isotopic-spin dependence of the reaction mechanism.

#### ${}^9\text{Be}(p,d){}^8\text{Be}$

The energy spectra from the reaction  ${}^9\text{Be}(p,d){}^8\text{Be}$  (Figs. 7 and 8) show deuteron groups corresponding to strongly excited levels of  ${}^8\text{Be}$  at 0.0, 3.1, 11.4, 16.95, 17.62, 18.18, and 19.21 MeV. A very small yield was observed for excited states of  ${}^8\text{Be}$  at 16.6 and 19.15 MeV. The first three levels of  ${}^8\text{Be}$  can be understood, at least qualitatively, by a cluster model of two  $\alpha$

<sup>21</sup> S. T. Butler, Phys. Rev. 106, 272 (1957).

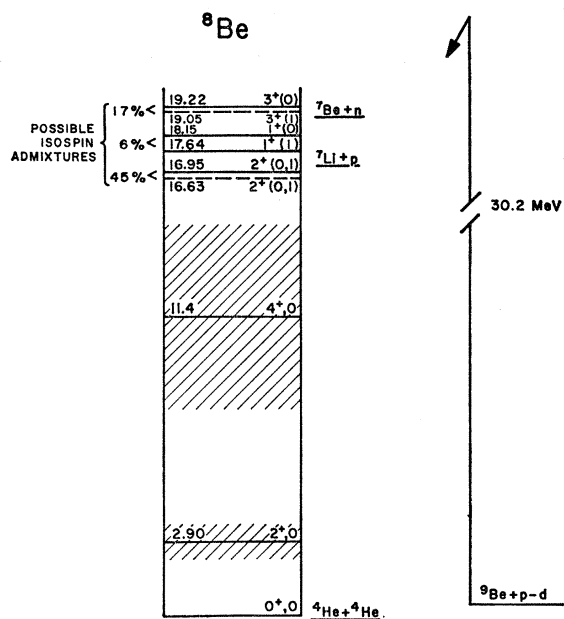


FIG. 9. Energy-level diagram of  ${}^8\text{Be}$ . The levels drawn in with dashed lines are those weakly excited in the  ${}^9\text{Be}(p,d){}^8\text{Be}$  reaction while those drawn in with the solid lines correspond to strongly excited levels. Also shown are the isospin admixtures which have been calculated for  $J^\pi=2^+$ ,  $1^+$ , and  $3^+$  doublets (Ref. 14).

particles excited into the rotational sequence  $0^+$ ,  $2^+$ , and  $4^+$  (Fig. 9).<sup>22</sup> Measurements of the differential cross section for the 11.4-MeV state ( $J^\pi=4^+$ ) were made from  $40^\circ$  to  $140^\circ$  in the lab with a large uncertainty due to the width of the state ( $\Gamma\sim 7$  MeV)<sup>7</sup> and a high background. The data show little structure in this range, the average value of the cross section falling between 0.02 and 0.05 mb/sr MeV at the resonance. The angular distribution does not exhibit the forward peaking characteristic of a direct reaction, since the peak could not be seen at angles less than  $35^\circ$ . This leads to the conclusion that this state is excited principally by a compound nucleus mechanism and not by a direct process in which some  $1f$  admixture in the ground state of  ${}^9\text{Be}$  contributes to the cross section.<sup>10</sup>

The next set of known levels of  ${}^8\text{Be}$  appear in the region of the  ${}^7\text{Li}+p$  and  ${}^7\text{Be}+n$  separation energies (Fig. 9). Previous experimental evidence has established the fact that isospin mixing is present within each of the three doublets ( $J^\pi=2^+$ ,  $1^+$ , and  $3^+$ ) in this region of excitation energy.<sup>23-27</sup> Wave functions for these doublet states have been calculated by mixing intermediate-coupling shell-model wave functions of pure isospin with a charge-dependent interaction.<sup>12</sup> The

<sup>22</sup> K. Wildermuth, Nucl. Phys. 31, 478 (1962).

<sup>23</sup> J. B. Marion, Phys. Letters 14, 315 (1965).

<sup>24</sup> C. P. Browne and J. R. Erskine, Phys. Rev. 143, 683 (1966).

<sup>25</sup> P. Paul, Z. Naturforsch. 21, 914 (1966).

<sup>26</sup> P. Paul, D. Kohler, and K. A. Snover, Bull. Am. Phys. Soc. 11, 26 (1966).

<sup>27</sup> G. T. Garvey, J. Cerny, and H. Pugh, Bull. Am. Phys. Soc. 11, 26 (1966).

TABLE I. Experimental cross section ratios and isospin admixtures calculated by Barker<sup>a</sup> for the  $J=1^+$ ,  $2^+$ , and  $3^+$  doublets.

Doublet	Ratio of cross sections (34 MeV)	Ratio of cross sections (41 MeV) <sup>b</sup>	Isospin admixtures <sup>c</sup> (amplitude squared) as calculated by Paul <sup>a</sup>
(16.6)/(16.9)	<1/20	1/25	45%
(17.6)/(18.2)	2.6	3.5	6%
(19.1)/(19.2)	<1/20		17%

<sup>a</sup> Reference 14.

<sup>b</sup> Reference 28.

<sup>c</sup> 50% admixture represents a doublet with maximal isospin mixing and 0% a doublet with states of pure isospin.

mixing coefficients were obtained by fitting existing experimental data and are given in Table I. The ratio of spectroscopic factors  $S(16.6)/S(16.9)$  calculated using this model is  $1/45$ ,<sup>14</sup> whereas the ratio obtained experimentally is less than  $1/20$ .

Some indication of the amount of isospin mixing within the doublets can be obtained if the single-particle cluster model is used to describe the states.<sup>23</sup> In this case, the  $(p,d)$  reaction will excite only one

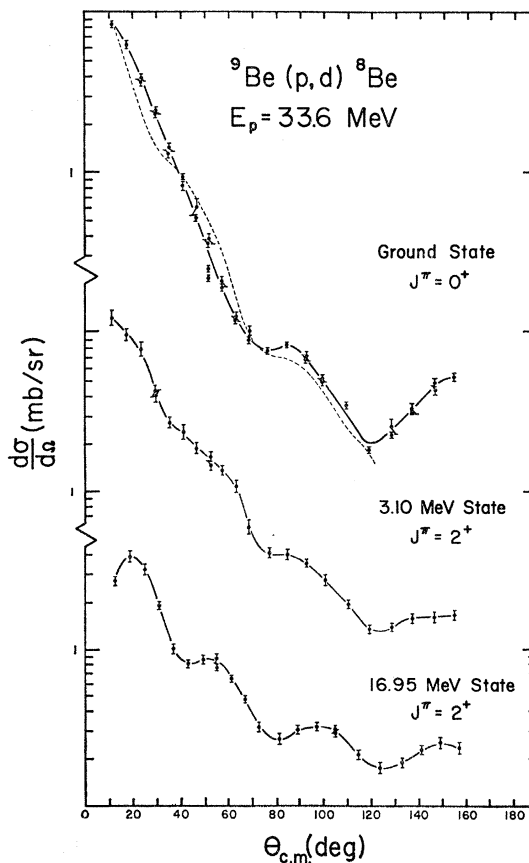


FIG. 10.  ${}^9\text{Be}(p,d){}^8\text{Be}$  angular distributions for the 0.0, 3.1, and 16.95-MeV states of  ${}^8\text{Be}$ . The DWBA fit to the ground-state differential cross section is shown with a dashed line.

member of the doublet if the pair is maximally mixed in isospin (50%). Conversely, if the members of the doublet are states of pure isospin ( $T=0$  or  $1$ ), both states should be observed by the  $(p, d)$  reaction with the same yield. Table I shows the data to be in general agreement with this simple model. The experimentally measured widths for the 16.95- and 19.21-MeV deuteron groups of  $103 \pm 15$  and  $208 \pm 30$  keV, respectively, are in agreement with the previously obtained values<sup>7</sup> of  $83 \pm 10$  and  $190$  keV, insuring that only one of the states in these doublets is strongly excited. The experimentally obtained cross-section ratios for these doublets are in agreement with those obtained at  $E_p = 40$  MeV.<sup>28</sup>

The angular distributions for all strongly excited states of  ${}^8\text{Be}$  (except for the above-mentioned  $4^+$  state) exhibit the characteristic shape for  $l_n=1$  pickup (Figs. 10 and 11). The differential cross section measurements for these states are in reasonable agreement with those obtained for  $E_p = 36$  MeV.<sup>29</sup> The relative flattening of the differential cross sections as the excitation energy of the state increases is a  $Q$ -value effect and was reproduced in the distorted-wave Born-approximation (DWBA) calculations.

#### DWBA ANALYSIS

Angular distributions for the elastically scattered protons from targets of  ${}^6\text{Li}$ ,  ${}^7\text{Li}$ , and  ${}^9\text{Be}$  were measured from  $12^\circ$  to  $130^\circ$  in the lab with an incident proton energy of 33.6 MeV. In the case of  ${}^7\text{Li}$ , the proton groups corresponding to the ground state and the 0.48-MeV state of  ${}^7\text{Li}$  could not be resolved. Angular distributions for both states had been measured at  $E_p = 25$  MeV<sup>30</sup> and the same relative yields were assumed in computing the differential cross section for the ground state of  ${}^7\text{Li}$  at  $E_p = 33.6$  MeV. This amounted to an average correction of 2% at forward angles and between 15% and 25% at backward angles.

The ABACUS computer code,<sup>31</sup> which employs a least-squares criterion, was used to fit the experimental distributions with an optical potential of the form

$$U_c - Vf(r, R, a_R) - iA_I W \frac{d}{dr} f(r, R, a_I) - \left( \frac{1}{mc} \right)^2 \frac{V_{so}}{r} \frac{d}{dr} f(r, R, a_R).$$

Here

$$f(r, R, a) = 1/e^{x+1}; \quad x = r - RA^{1/3}/a,$$

and  $U_c$  is the Coulomb potential from a uniformly

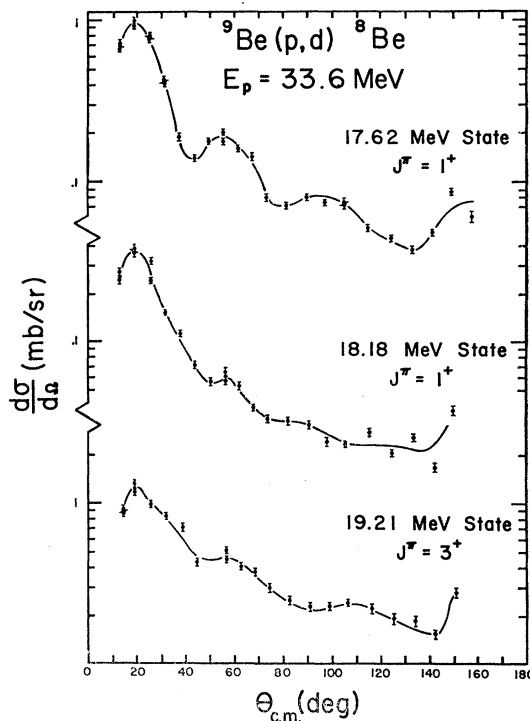


FIG. 11.  ${}^9\text{Be}(p, d){}^8\text{Be}$  angular distributions for the 17.62-, 18.18-, and 19.21-MeV states of  ${}^8\text{Be}$ .

charged sphere of radius  $RA^{1/3}$  F. A compilation of the optical parameters obtained for proton scattering is given in Table II.

Data for the elastic scattering of deuterons from  ${}^9\text{Be}$  at  $E_d = 27.7$  MeV<sup>32</sup> and from  ${}^7\text{Li}$  at  $E_d = 28$  MeV<sup>33</sup> were also fitted by an optical potential using the ABACUS code; the parameters obtained are given in Table III. No spin-orbit term was included in the optical potential and the imaginary diffuseness ( $a_I$ ) was set equal to the real diffuseness ( $a_R$ ).

The DWBA analysis was carried out using the Masefield computer code. Geometry parameters for the picked-up neutron were  $a_n = 0.65$  F and  $R_n = 1.25A^{1/3}$  F. No spin-orbit term was included in the neutron potential.

The DWBA calculations led to an interesting result, in that it was impossible to get a reasonable fit to the  $(p, d)$  angular-distribution data using the optical parameters in Tables II and III. However, if the imaginary

TABLE II. Proton optical parameters.

Target	$V$ (MeV)	$W$ (MeV)	$V_{so}$ (MeV)	$R$ (F)	$a_R$ (F)	$a_I$ (F)
${}^6\text{Li}$	44.56	6.92	7.38	1.124	0.578	0.685
${}^7\text{Li}$	46.45	6.34	7.18	1.187	0.478	0.727
${}^9\text{Be}$	48.92	6.44	6.30	1.139	0.613	0.616

<sup>28</sup> J. B. Marion and C. A. Ludemann, Bull. Am. Phys. Soc. 11, 26 (1966).

<sup>29</sup> I. Slaus (private communication).

<sup>30</sup> G. Grawley and S. Austin, International Conference on Nuclear Physics, Gatlinburg, 1966 (unpublished).

<sup>31</sup> E. H. Auerbach, Brookhaven National Laboratory Report No. BNL6562, ABACUS-2, 1962 (unpublished).

<sup>32</sup> R. J. Slobodrian, Phys. Rev. 125, 1003 (1962).

<sup>33</sup> R. J. Slobodrian, Nucl. Phys. 32, 684 (1962).

TABLE III. Deuteron optical parameters.

Target	$V$ (MeV)	$W$ (MeV)	$R$ (F)	$a_R$ (F)
${}^7\text{Li}^a$	79.45	11.23	1.094	0.769
${}^9\text{Be}$	74.03	11.67	1.239	0.736

<sup>a</sup> Data renormalized by 0.85.

well of the deuteron optical potential ( $W_d$ ) is increased by a factor of three in the case of  ${}^9\text{Be}(p,d){}^8\text{Be}$  and a factor of 4 in the cases of  ${}^7\text{Li}(p,d){}^6\text{Li}$  and  ${}^6\text{Li}(p,d){}^5\text{Li}$ , reasonable fits are obtained in all cases (Figs. 4, 6, 10). A 20% variation of any of the other parameters would not produce similar results. The same situation was encountered in applying a DWBA analysis to the data from  ${}^4\text{He}(p,d){}^3\text{He}$  with  $E_p = 31$  MeV.<sup>34</sup>

This anomalously large value of  $W_d$  may be a consequence of using the optical-model potential to describe the interaction of the scattered deuteron with a relatively small number of nucleons which comprise the scattering nucleus. It may also be due to the fact that in the optical model, the deuteron is treated as a point particle, whereas the weak coupling within the deuteron itself is likely to be sensitive to deformations caused by interactions with the target nucleus. No similar effect was noted, however, when optical parameters obtained from elastic scattering were used in DWBA calculations of the  $(p,d)$  reaction with heavier nuclei.<sup>11</sup> Thus it appears that the first possibility may be the more relevant of the two.

### SPECTROSCOPIC FACTORS

The experimental spectroscopic factor  $S_{A \rightarrow B}$  for the transition  $A(p,d)B$ , which proceeds by a direct pickup of  $1p_{3/2}$  and  $1p_{1/2}$  neutrons, was calculated from the expression

$$S_{A \rightarrow B} = \sigma_{\text{EXP}} / 1.6 \sigma_{\text{DWBA}}^M,$$

$\sigma^M$  is the magnitude of the differential cross section at

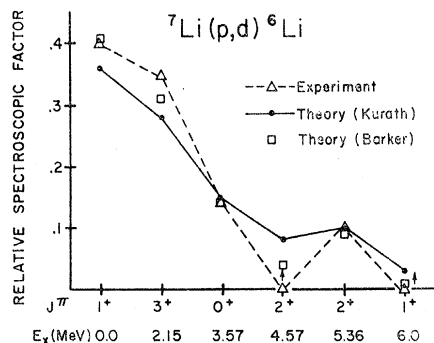


FIG. 12. Comparison of theoretical and experimental relative spectroscopic factors for  ${}^7\text{Li}(p,d){}^6\text{Li}$ . The arrows above the levels at 4.57- and 6.0-MeV excitation energy are used to indicate that small deuteron yields from these levels may not have been observed because of the width of these states and a high background.

<sup>34</sup> S. M. Bunch, H. H. Foster, and C. C. Kim, Nucl. Phys., 53, 241 (1964).

the angle for which it has its characteristic  $l_n=1$  maximum. The DWBA result, which uses the zero-range approximation, is multiplied by a factor of 1.6 to make it approximately equivalent to a calculation using the effective-range theory.<sup>35,36</sup>

The theoretical spectroscopic factors were obtained for the transition  $A(p,d)B$  from the coefficients of fractional parentage,  $\beta_{ij}$ , calculated by Kurath using the intermediate-coupling model for  $1p$  shell nuclei.<sup>21</sup> The theoretical spectroscopic factor  $S_{A \rightarrow B}$  is given by

$$S_{A \rightarrow B}(l_n=1; j_n=\frac{3}{2}, \frac{1}{2}) = n(T'_{\frac{1}{2}} M_{T'_{\frac{1}{2}}} | T M_T)^2 \sum_{j=\frac{1}{2}, \frac{3}{2}; l=1} \beta_{ij}^2,$$

$n$  is the number of nucleons in the  $1p$  shell of  $A$  and  $(|)$  is a Clebsch-Gordan coefficient with  $T', M_{T'}$  and  $T, M_T$ ; the isotopic spin and its projection for the final state and initial state, respectively. As calculated above, the spectroscopic factors relate to states with pure isospin. Another set of spectroscopic factors for the reaction  ${}^7\text{Li}(p,d){}^6\text{Li}$  was obtained from the shell-model calculations of Barker.<sup>14</sup>

Theoretical and experimental relative spectroscopic factors were obtained by normalizing the sum of the spectroscopic factors for each reaction to 1. Considering the difficulty in extracting meaningful absolute spectroscopic factors from the DWBA comparison to the data, the relative spectroscopic factor was calculated to provide a better look at the relative amount of overlap between the target nucleus's ground-state wave function and the wave functions of the residual nucleus's different excited states plus a  $1p$ -shell neutron. The comparisons of experimental results to theoretical calculations are shown for  ${}^7\text{Li}(p,d){}^6\text{Li}$  and  ${}^9\text{Be}(p,d){}^8\text{Be}$  in Figs. 12 and 13(a).

The agreement between theory and experiment for  ${}^7\text{Li}(p,d){}^6\text{Li}$  is good. The experimental spectroscopic factors of zero for the 4.57- and 6.0-MeV states could be due to the difficulty in extracting the small deuteron yields, corresponding to these broad states, from the background.

Figure 13(a) shows the large discrepancy between theory and experimental spectroscopic factors for the  ${}^8\text{Be}$   $J^\pi=2^+$  doublet at 16.6 and 16.9 MeV and also for the  $J^\pi=3^+$  doublet at 19.1 and 19.2 MeV. This disagreement could result from the fact that the experimental spectroscopic factors have been extracted using a DWBA calculation with deuteron potential parameters obtained from the elastic scattering of deuterons from the ground state of  ${}^9\text{Be}$ , whereas the nucleus is actually left in a state 17 to 19 MeV in excitation above the ground state of  ${}^9\text{Be}$ . The effect of this approximation on the extraction of the spectroscopic factor is not known, but it should be noted that the same large discrepancies are not present in the results for the

<sup>35</sup> R. Satchler (private communication).

<sup>36</sup> N. Austern, in *Fast Neutron Physics*, edited by J. B. Marion and J. L. Fowler (Interscience Publishers Inc., New York, 1961), Vol. II.

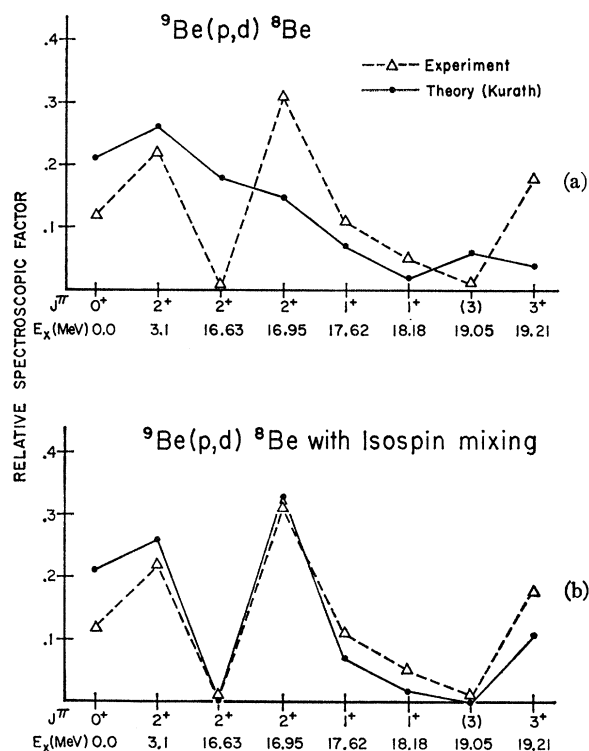


FIG. 13. Comparison of theoretical and experimental relative spectroscopic factors for  ${}^9\text{Be}(p,d){}^8\text{Be}$ . Good agreement is obtained except for the  $J^\pi = 2^+$  and  $3^+$  doublets. If the sum of the theoretical spectroscopic factors within these doublets in (a) is fixed, but the ratio of strengths is adjusted to best fit the experimental data, (b) is obtained. This is equivalent to mixing states with definite isospin within the doublets.

$J^\pi = 1^+$  doublet at 18 MeV excitation. This last observation fits in with another possible explanation for the observed disagreement. The theoretical calculations assume the states to be pure in isotopic spin, whereas previous experiments have shown considerable isospin mixing to be present within the  $J^\pi = 2^+$  and  $3^+$  doublets. If two states of pure isospin are mixed to produce two new final states of indefinite isospin, the ratio of spectroscopic factors for the isospin mixed pair will be different, in general, from that originally found for the pair with pure isospin. However, the sum of the spectroscopic factors for each pair is the same for both cases. Assuming, therefore, that the experimental results only represent a mixing of the theoretical isospin pure states, there should be agreement between theoretical and experimental sums of spectroscopic factors for each doublet. The sum of the experimental

spectroscopic factors for the  $J^\pi = 2^+$  and  $3^+$  doublets is 0.32 and 0.19, respectively, whereas the sum of the theoretical spectroscopic factors for the same  $J^\pi = 2^+$  and  $3^+$  doublets is 0.33 and 0.11, respectively. This same approach was also used in obtaining Fig. 13(b) where the ratio of spectroscopic factors within the  $J^\pi = 2^+$  and  $3^+$  doublets has been adjusted to give better agreement with experiment, while the sum of spectroscopic factors within the doublets is the same as that in Fig. 13(a). Thus, good agreement with theory can be obtained, assuming that the isospin mixing with the  $J^\pi = 2^+$  and  $3^+$  doublets is the cause of the major differences observed.

### SUMMARY

In general, there is relatively good agreement between experimentally obtained relative spectroscopic factors and the calculations of Kurath<sup>13</sup> and of Barker.<sup>14</sup> The inclusion of isotopic-spin mixing within the  $J^\pi = 2^+$  and  $3^+$  doublets of  ${}^8\text{Be}$  resolves the large difference between experiment and theory for these cases. In fact, considering the good agreement obtained between theory and experiment in the case of  ${}^7\text{Li}(p,d){}^6\text{Li}$ , the discrepancies noted in the  ${}^9\text{Be}(p,d){}^8\text{Be}$  reaction illustrate in a very concise manner that the wave functions of the  ${}^8\text{Be}$   $2^+$  and  $3^+$  states contain admixtures of  $T=0$  and  $T=1$ . With this modification, the intermediate-coupling model appears to give a satisfactory picture of lower  $1p$ -shell nuclei with regard to spectroscopic factors obtained by  $(p,d)$  reactions.

No evidence was found for any  $2s-1d$  shell admixtures in the ground-state wave functions of  ${}^6\text{Li}$ ,  ${}^7\text{Li}$ , and  ${}^9\text{Be}$ , and the strongly excited 16.6-MeV state of  ${}^6\text{Li}$  is the only case where neutron pickup from the  $1s$  shell was observed with any appreciable yield. The 11.4-MeV state of  ${}^8\text{Be}(J^\pi = 4^+)$  appears to be excited by a compound nucleus mechanism and not because of any  $1f$  admixture in the  ${}^9\text{Be}$  ground-state wave function.<sup>10</sup> From this study, therefore, the ground states of  ${}^6\text{Li}$ ,  ${}^7\text{Li}$ , and  ${}^9\text{Be}$  appear to consist of tightly bound  $1s$  cores, the remaining nucleons residing in the  $1p$  shell with no sizable admixtures from other shells.

### ACKNOWLEDGMENTS

The author is indebted to Professor E. Kashy for suggesting this work and for helpful discussions of the results. Many thanks go to R. L. Kozub and P. Plauger for assistance in taking data.